Supporting Information

Crystal Structure Analysis, Stability, Phase Transformation and Selective Nucleation Mechanism of Fluralaner Polymorphs

Guangyan Li[1], Ting Wang[1,2], Xin Huang[1,2,3], Na Wang[1,2]*, Lina Zhou[1,2], Beiqian Tian[1], Ziwei Feng[1], Ailing Liu[4], Yaling Li[4] and Hongxun Hao[1,2]*

1 National Engineering Research Center of Industrial Crystallization Technology, School of Chemical Engineering and Technology, Tianjin University, Tianjin 300072, China; 2020207362@tju.edu.cn (G.L.); wang_ting@tju.edu.cn (T.W.); linazhou@tju.edu.cn (L.Z.); beiqiantian@tju.edu.cn (B.T.); 2020207427@tju.edu.cn (Z.F.); hongxunhao@tju.edu.cn (H.H.)

2 Collaborative Innovation Center of Chemical Science and Engineering (Tianjin), Tianjin 300072, China.

3 Zhejiang Institute of Tianjin University, Ningbo 311305, China.

4 Tianjin Ringpu Bio−technology Co Ltd, Tianjin 300072, China

* Corresponding author email: x_huang@tju.edu.cn (X.H.); wangna224@tju.edu.cn (N.W.)

Table S1. Experimental and simulated PXRD pattern peak positions (°) and relative

intensities (%) of Form I, Form II and Form III.

Form I (exp)		Form II (exp)		Form III (exp)		Form I (calc)		Form II(calc)		Form III (calc)	
2θ	I%	2θ	I%	2θ	I%	2θ	I%	2θ	I%	2θ	I%
4.281	66.4	9.339	1.3	4.181	20	4.421	100	9.359	7.8	4.4	100
4.561	1.2	10.16	9.3	8.519	24.5	8.859	20.9	10.2	45.5	8.802	28.5
8.621	49.7	10.599	5.4	10.881	9	11.3	11.9	10.581	4.1	11.261	13.6
11.019	6.9	11.24	5.4	12.477	1.9	12.8	5.8	11.28	23.7	12.818	9.5
12.521	0.9	11.8	4.1	12.859	4.4	13.299	1.8	11.8	13.8	13.221	2.6
12.999	7.4	12.22	16.3	13.543	3.7	13.741	6.5	12.26	58.7	14.04	10.6
13.46	1.7	13.281	1.5	14.239	21.1	14.041	9.1	13.321	3.2	14.72	36.8
14.36	4.7	14.74	27.7	14.541	7.8	14.738	30.7	14.781	59	14.94	11.2
14.681	5	15.241	5.7	16.099	9.1	14.978	5.1	15.3	17	16.6	15.8
16.219	3.7	15.92	15.8	16.62	13.2	15.542	2.2	15.599	3.7	17.121	49.6
16.76	6	16.9	4.3	17.24	16.8	16.361	4.1	15.901	13.8	17.699	50.4
17.581	5.1	17.921	4.5	18.54	15	16.621	13.8	16.999	9.3	17.918	27.5
17.979	2.9	18.48	28.9	19.22	10.4	17.1	28.2	17.519	3.3	19.022	9.7
18.7	18.6	20.06	57.7	19.699	6.6	17.659	9.9	17.978	12.9	19.599	35.5
19.299	8.9	20.419	17.5	20.94	100	17.959	11	18.519	41.5	20.098	26.9
21.08	56.7	21.299	98	21.621	58.3	18.38	10.4	18.781	19.1	21.561	86
21.8	100	21.859	11.2	22.099	27.3	19.119	6.4	19.441	2.8	22.139	25.8
22.221	18.7	22.66	22.9	22.7	9.4	19.601	30	20.1	100	22.642	56.3
22.881	25.1	23.179	11.5	23.66	13.1	20.098	1.2	20.5	42.5	23.241	7.6
23.281	1	24.002	1.8	24.24	19.3	20.399	2.3	20.92	11	23.739	13.4
23.76	6.9	24.62	9.4	24.72	42.4	20.702	6.6	21.301	51.3	24.181	76.9
24.36	8.1	25.64	11.9	26.059	60.7	20.94	8.7	21.898	37	24.741	41.2
24.879	57.4	26.1	28.5	26.96	22.4	21.56	82.5	22.261	19.3	25.261	47.3
26.24	78.4	26.7	100	27.5	8.1	22.242	23	22.663	21.8	25.781	4.7
27.159	16.9	27.52	3.8	28.719	6.6	22.7	29.4	23.259	18.2	26.501	44.3
27.659	6.8	28.24	15.6	29.561	13.7	23.379	14.1	23.6	3.3	26.9	20.8
28.5	1.7	28.839	3.6	30.04	4.9	23.741	5.4	24.06	3	27.459	10.9
28.861	6	30.179	6.7	30.6	3	24.24	43.8	24.661	21.8	27.66	17
29.48	5.3	30.68	6.9	31.28	11	24.799	24.8	25.62	14.9	28.12	9.6
29.74	5.4	31.74	3	32.84	10.2	25.36	36.1	26.119	35.5	29.32	21.9
30.181	2.2	32.22	5.1	34.98	7.4	26.081	2.2	26.719	52.3	29.721	3.8
31.021	1.9	33.46	2.2	37.139	6	26.56	37.7	27.362	4.5	30.001	11.3
31.521	8.3	34.28	3.8	38.439	3.9	26.779	21.7	27.558	9.4	30.338	33.9
33.059	14.5	35.439	2.1	39.081	2.9	26.979	10	28.26	15.3	30.579	7.7
35.299	3.7	36.02	2.1			27.501	7.4	28.861	8	30.78	4
35.999	2.3	36.98	5.3			27.721	11.2	29.659	3	31.322	9.5
36.88	2.3	37.741	1.5			28.2	7.3	30.2	7.9	31.96	9.9
37.299	3.5	38.839	3.1			28.981	6.5	30.719	8.8	32.96	7.9
38.541	1.1					29.421	11	30.92	6	33.2	13.6
39.539	3.8					30.021	9.1	31.299	5.7	33.522	8.1

			30.28	10.3	31.701	5.2	34.099	5.8
			30.681	5.9	32.221	11.1	34.658	1.7
			31.218	1.3	33.139	3.1	35.021	1.6
			31.58	3.6	33.4	3.5	35.818	12
			32.121	5.9	33.78	3.6	36.28	4.3
			32.482	0.9	34.321	5.7	36.901	3.9
			33.28	4.3	35.161	3.7	37.259	2.6
			33.68	6.4	35.481	4.1	37.579	14.2
			34.02	5.1	36.081	5.8	38.1	10.1
			34.86	3.4	36.401	2.5	39.159	8.6
			35.94	3.6	37.061	10.4	39.999	8.6
			36.419	9.3	37.419	3.3		
			36.98	2	37.801	4.4		
			37.64	6.7	38.301	3.5		
			38.159	4.7	38.939	5.9		
			39.32	2.5	39.26	2.5		
					39.801	2.5		

Table S2. Hydrogen bonds in crystal structures of Form I, Form II and Form III of fluralaner.

	D-H···A	d(D-H), Å	d(H···A), Å	d(D-A), Å	∠(DHA), deg.
Form I	N2-H2···O2	0.880	1.961	2.796	157.70
	C12-H12···C15	0.950	2.860	3.764	159.41
	C17-H17B···O3	0.990	2.347	3.224	147.06
	N3-H3···O3	0.880	2.638	3.158	118.86
	N2-H2···O2	0.880	1.963	2.786	155.24
	C4-H4···F5	0.951	2.926	3.107	91.95
	C8-H8A···F5	0.990	2.531	3.517	173.58
	C15-H15···O2	0.950	2.526	3.419	156.54
	N3-H3···N1	0.880	2.527	3.222	136.45
	C19-H19B···O1	0.990	2.368	3.154	135.85
Form II	N3-H3···O2	0.902	2.182	3.021	154.45
	C19-H19A···C14	0.970	2.597	3.552	168.36
	C17-H17A···C14	0.970	2.821	3.675	147.29
	C17-H17A···C15	0.970	2.882	3.601	131.72
	C8-H8A···O3	0.970	2.327	3.229	154.59
	N3-H3···O2	0.893	2.209	3.036	153.81
	C22-H22···N1	0.960	2.723	3.594	151.27
	C4-H4···O3	0.930	2.445	3.301	153.16
	C17-H17···O1	0.970	2.874	3.212	101.59
	N2-H2···N1	0.898	2.363	3.108	140.44
Form III	N2-H2···O2	0.880	1.967	2.798	156.80

C12-H12···C15	0.950	2.892	3.795	159.14
C17-H17B···O3	0.990	2.335	3.211	147.06
N3-H3···O3	0.881	2.589	3.125	120.03
C4-H4···F5	0.950	2.971	3.145	91.65
C8-H8A···F5	0.990	2.499	3.486	174.57
C15-H15···O2	0.950	2.538	3.422	154.73
N3-H3···N1	0.881	2.528	3.225	136.49
C19-H19B···O1	0.991	2.388	3.165	134.77

Table S3. The detailed data of torsion angles.

Torsion angle (°)	Form I-S	Form I-R	FormII-R1	FormII-R2	Form III
Cl1−C1−C2−C3	-179.4(2)	178.8(2)	179.3(3)	179.5(4)	179.5(4)
Cl1−C1−C6−C5	-179.7(2)	-179.4(2)	179.6(3)	179.4(3)	-179.9(4)
Cl2−C3−C4−C5	-178.4(2)	178.0(2)	176.7(3)	178.5(4)	177.6(4)
O1−N1−C9−C8	1.3(4)	-1.3(4)	2.5(5)	1.3(5)	-1.4(6)
O1−N1−C9−C10	-178.0(3)	176.8(3)	-179.5(3)	-179.6(3)	177.1(4)
O1−C7−C8−C9	4.5(3)	-3.6(3)	6.3(4)	6.9(4)	-2.9(5)
O1−C7−C21−F1	-60.7(3)	57.9(3)	60.4(5)	59.2(5)	58.6(5)
O1−C7−C21−F2	179.0(2)	179.8(2)	179.8(4)	-179.6(3)	179.8(4)
O1−C7−C21−F3	60.4(4)	-61.5(3)	-60.0(5)	-58.6(5)	-60.8(5)
N1−O1−C7−C5	119.2(3)	-119.6(2)	-130.6(3)	-131.5(3)	-121.0(4)
N1−O1−C7−C8	-4.2(3)	3.2(3)	-5.5(4)	-6.8(4)	2.4(5)
N1−O1−C7−C21	-122.4(3)	120.8(3)	109.5(4)	109.7(3)	119.7(4)
N1−C9−C10−C15	-1.5(5)	1.6(5)	3.7(6)	4.3(6)	1.2(8)
N1−C9−C10−C11	175.8(3)	-176.3(3)	-176.7(4)	-174.6(4)	-176.9(5)
N2−C17−C18−O3	-93.2(4)	90.6(3)	167.3(3)	165.5(4)	92.0(6)
N2−C17−C18−N3	84.0(3)	-86.7(3)	-13.0(5)	-16.1(6)	-85.3(5)
N3−C19−C20−F4	55.2(4)	-54.7(4)	-57.7(5)	-58.2(5)	-55.6(6)
N3−C19−C20−F5	174.8(3)	-174.9(3)	-177.2(4)	-178.0(3)	-174.5(4)
N3−C19−C20−F6	-65.1(4)	66.3(4)	61.6(6)	62.2(5)	67.0(6)
C1−C2−C3−Cl2	177.8(2)	-177.5(2)	-177.4(3)	-179.0(4)	-177.0(4)
C1−C2−C3−C4	-1.3(5)	1.2(5)	-0.1(6)	0.0(9)	0.6(8)
C2−C1−C6−C5	-0.3(5)	0.5(5)	-0.2(6)	-0.7(7)	0.4(8)
C2−C3−C4−C5	0.6(4)	-0.7(4)	-0.7(6)	-0.5(9)	0.0(8)
C3−C4−C5−C6	0.2(4)	0.1(4)	1.0(5)	0.4(7)	-0.4(7)
C3−C4−C5−C7	179.7(3)	178.7(3)	-177.5(3)	-179.3(4)	-179.1(4)
C4−C5−C6−C1	-0.4(4)	0.0(4)	-0.6(5)	0.1(6)	0.2(7)
C4−C5−C7−O1	-171.7(2)	171.3(2)	134.5(3)	142.5(4)	171.8(4)
C4−C5−C7−C8	-53.8(4)	53.7(4)	17.4(5)	25.3(6)	54.1(6)
C4−C5−C7−C21	74.8(4)	-74.1(4)	-109.7(4)	-100.8(5)	-74.0(6)
C5−C7−C8−C9	-115.6(3)	116.6(3)	125.2(3)	126.1(4)	117.2(4)
C5−C7−C21−F1	56.4(4)	-60.3(4)	-56.7(6)	-58.2(5)	-59.2(6)

C5−C7−C21−F2	-63.9(4)	61.5(4)	62.8(5)	63.1(5)	62.0(6)
C5−C7−C21−F3	177.5(3)	-179.7(3)	-177.0(4)	-175.9(4)	-178.5(4)
C6−C1−C2−C3	1.1(5)	-1.1(5)	0.6(6)	0.6(8)	-0.8(8)
C6−C5−C7−O1	7.8(4)	-7.4(4)	-44.1(4)	-37.2(5)	-6.9(6)
C6−C5−C7−C8	125.7(3)	-125.0(3)	-161.1(3)	-154.5(4)	-124.6(5)
C6−C5−C7−C21	-105.7(3)	107.1(3)	71.8(4)	79.4(5)	107.3(5)
C7−O1−N1−C9	1.9(3)	-1.3(3)	2.2(4)	3.7(5)	-0.8(5)
C7−C5−C6−C1	-179.9(3)	178.7(3)	178.0(3)	179.9(4)	178.9(4)
C7−C8−C9−N1	-3.7(4)	3.1(4)	-5.7(4)	-5.4(5)	2.8(6)
C7−C8−C9−C10	175.6(3)	-174.9(3)	176.3(3)	175.6(4)	-175.7(5)
C8−C7−C21−F1	-173.9(3)	170.8(3)	172.1(4)	172.0(4)	171.3(4)
C8−C7−C21−F2	65.8(3)	-67.3(3)	-68.4(5)	-66.7(5)	-67.5(5)
C8−C7−C21−F3	-52.8(4)	51.4(4)	51.7(5)	54.3(5)	51.9(6)
C8−C9−C10−C15	-179.2(3)	179.5(3)	1.1(6)	4.3(6)	179.5(5)
C8−C9−C10−C11	-3.5(5)	1.6(5)	-178.5(4)	-176.8(4)	1.5(7)
C9−C10−C15−C14	177.6(3)	-178.2(3)	-178.8(3)	-178.7(4)	-178.1(5)
C9−C10−C11−C12	-177.1(3)	177.3(3)	-179.9(4)	-179.6(4)	177.6(5)
C10−C15−C14−C13	-0.3(6)	0.5(5)	-1.3(6)	-2.2(6)	0.2(8)
C10−C15−C14−C22	179.2(4)	179.6(4)	179.6(4)	178.6(4)	179.2(5)
C15−C10−C11−C12	-0.2(5)	-0.3(5)	0.5(6)	-0.7(7)	-0.5(7)
C15−C14−C13−C12	0.7(5)	0.1(5)	0.5(6)	0.4(6)	0.2(8)
C15−C14−C13−C16	-174.8(3)	175.3(3)	176.5(3)	177.2(4)	175.0(5)
C14−C13−C12−C11	0.2(5)	-1.0(5)	0.8(6)	1.2(7)	-0.8(8)
C14−C13−C16−O2	103.9(4)	-102.2(4)	-58.9(6)	-60.6(6)	-101.9(6)
C14−C13−C16−N2	-78.3(4)	78.9(4)	121.4(4)	118.9(4)	79.1(6)
C13−C12−C11−C10	-0.3(6)	0.5(5)	-1.3(6)	-1.0(7)	0.9(8)
C12−C13−C16−O2	-71.7(4)	73.2(4)	117.2(5)	116.2(5)	73.0(7)
C12−C13−C16−N2	106.1(3)	-105.7(3)	-62.4(5)	-64.3(5)	-106.0(6)
C11−C10−C15−C14	0.3(5)	-0.3(5)	0.8(6)	2.4(6)	0.0(8)
C16−N2−C17−C18	-95.8(3)	96.4(3)	137.2(4)	138.6(4)	96.8(6)
C16−C13−C12−C11	175.5(3)	-176.4(3)	-175.3(4)	-175.6(4)	-175.8(5)
C17−N2−C16−O2	-1.4(5)	1.0(5)	-8.2(7)	-7.8(6)	0.7(8)
C17−N2−C16−C13	-179.1(3)	179.9(3)	171.5(4)	172.7(3)	179.7(4)
C18−N3−C19−C20	98.5(4)	-96.9(4)	95.2(5)	96.2(4)	-98.3(6)
C19−N3−C18−O3	0.6(5)	-0.8(5)	-6.2(5)	-7.0(6)	-0.8(8)
C19−N3−C18−C17	-176.6(3)	176.5(3)	174.1(3)	174.8(4)	176.4(4)
C21−C7−C8−C9	116.4(3)	-115.5(3)	-106.4(4)	-107.5(4)	-114.7(4)
C22−C14−C13−C12	-179.1(4)	-179.0(4)	179.6(4)	179.6(4)	-178.8(5)
C22−C14−C13−C16	3.6(5)	-3.8(5)	-4.3(6)	-3.7(7)	-4.1(8)

Table S4. Torsion angles of various conformers.

Torsion angle(°)	Form I-R	Form II-R1	Form II-R2	Form III-R
N1-C9-C10-C15	1.6	-176.7	-174.6	1.2
C14-C13-C16-N2	78.9	121.4	118.9	79.1
C16-N2-C17-C18	96.4	137.2	138.6	96.8
N2-C17-C18-N3	-86.7	-13.0	-16.1	-85.3

Table S5. Molecular dynamics simulation details.

Number of molecules	Isopropanol solution	isopropanol/hexane solution
Isopropanol	500	125
n-hexane	0	375
Fluralaner (S)	5	5
Fluralaner (R)	5	5

Table S6. Thermal Data for Different Forms of Fluralaner Obtained by DSC.

	Form I	Form II	Form III
T_{onset} (℃)	175.24	171.38	165.07, 174.31
T_m (℃)	177.61	174.74	169.22, 176.31
enthalpy, ΔH_f (kJ/mol)	51.72	57.19	8.18, 45.68

Table S7. The results of cooling crystallization experiment.

Solvent	supersaturation	Form

methanol	1 ~ 4	I
ethanol	1 ~ 4	I
isopropanol	1 ~ 4	I
n-propanol	1 ~ 4	I
isopropanol/n-hexane(1:5 v/v)	1 ~ 4	III
n-propanol/n-hexane(1:5 v/v)	1 ~ 4	III

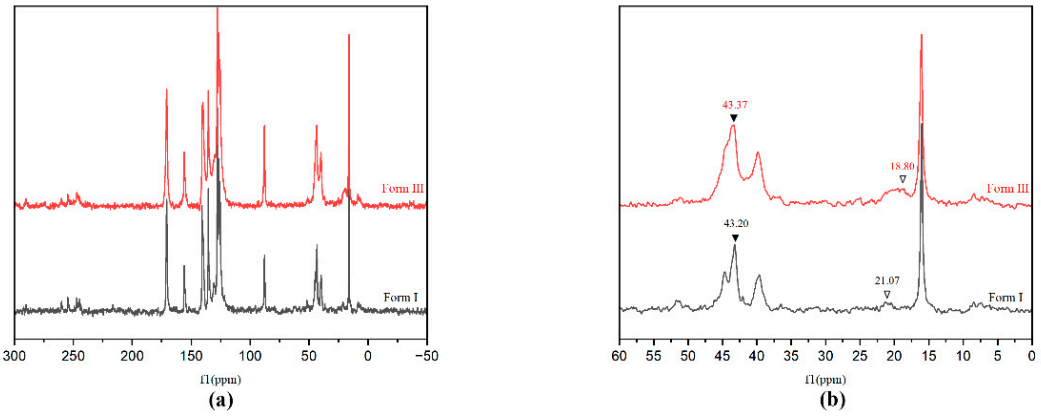

Figure S1. Solid-state NMR spectra of fluralaner Form I and Form III.

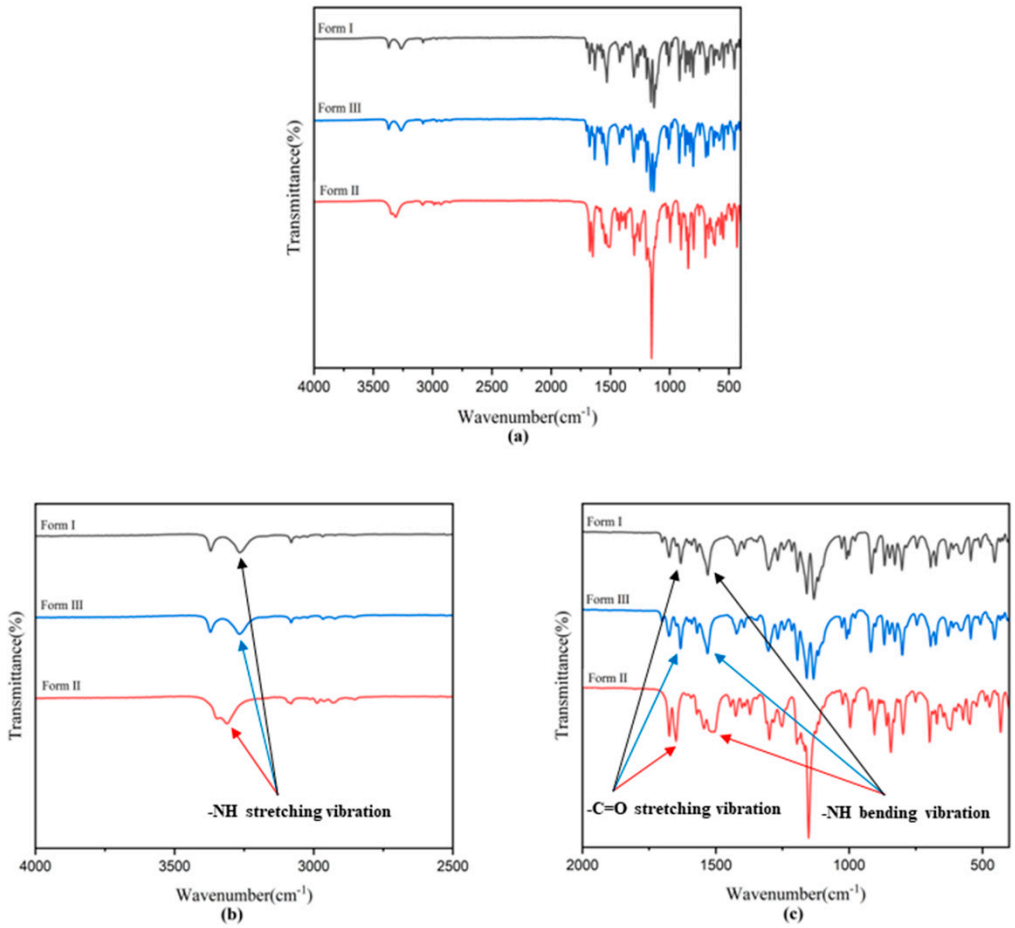

Figure S2. The FT-IR curves of Form I, Form II and Form III.

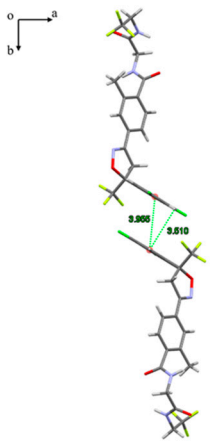

Figure S3. Weak π-π interactions in the crystal structure of Form I

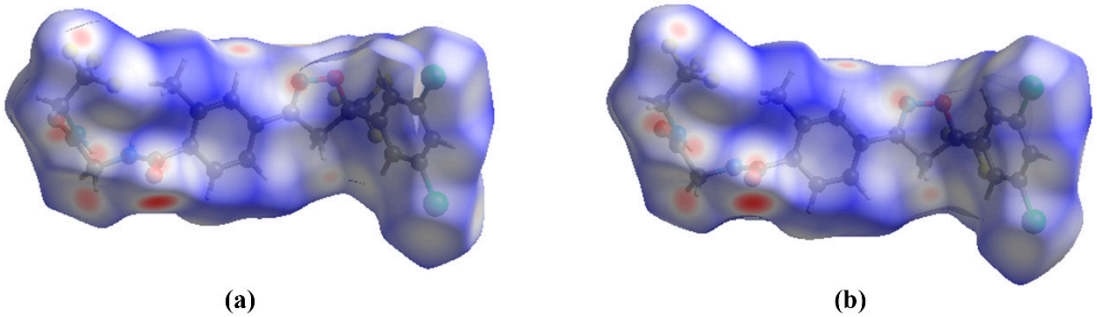

(a) (b)

Figure S4. A view of Hirshfeld surface mapped over d_{norm} for crystal forms of Fluralaner: (a) Form I, (b) Form III.

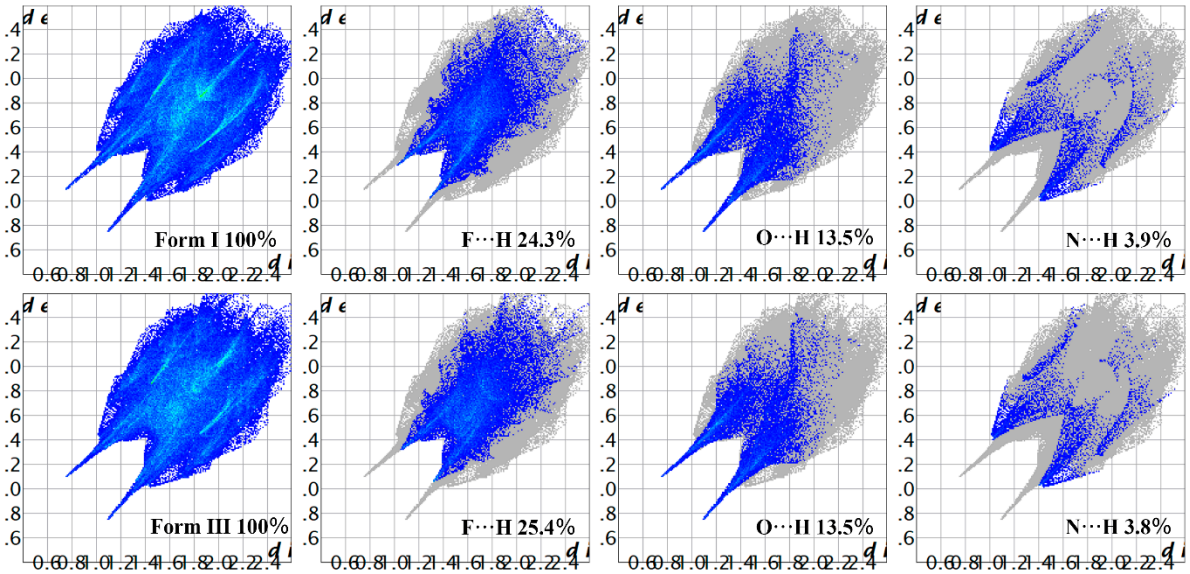

Figure S5. 2D Hirshfield fingerprint plots for Form I and Form III.

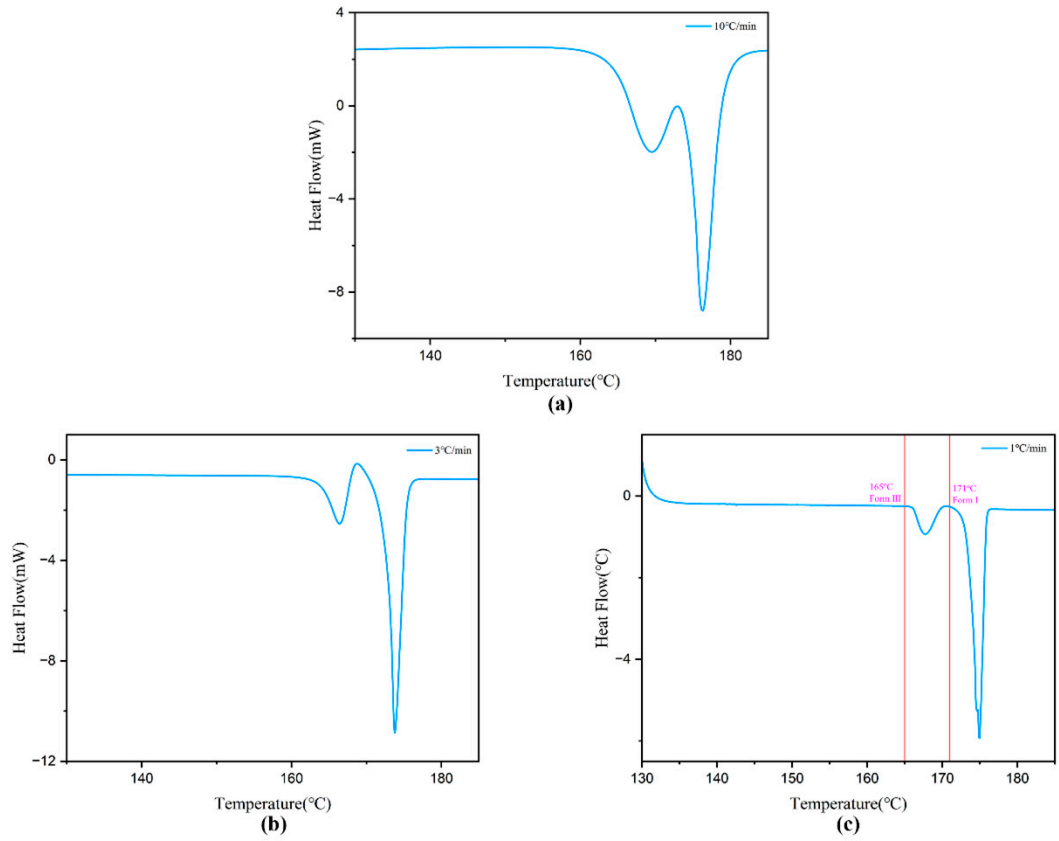

Figure S6. DSC curves of Form III at different heating rates,(a) 10℃/min, (b) 3/min, (c)1℃/min

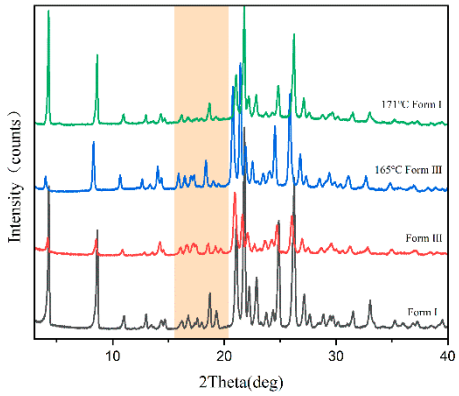

Figure S7. PXRD of Form III at different temperatures (165℃ and 171℃).

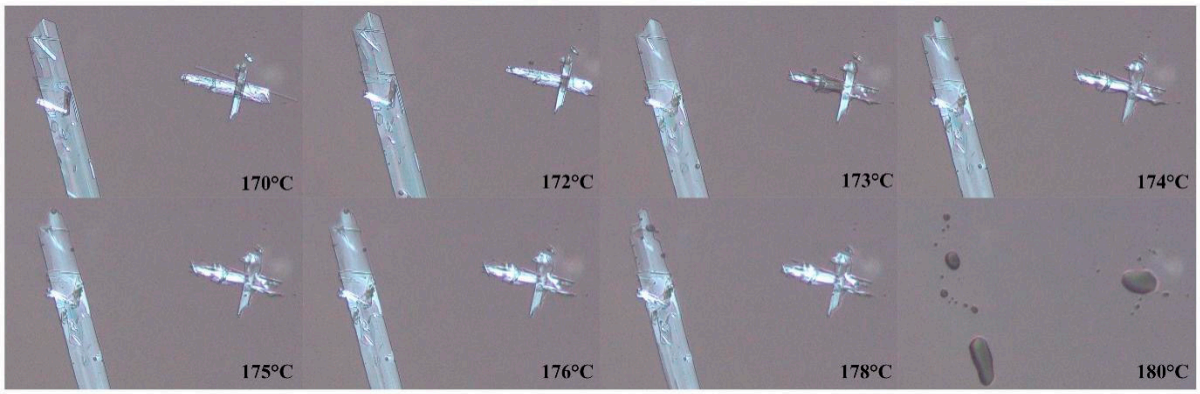

Figure S8. HSM images of Form III at different temperatures.

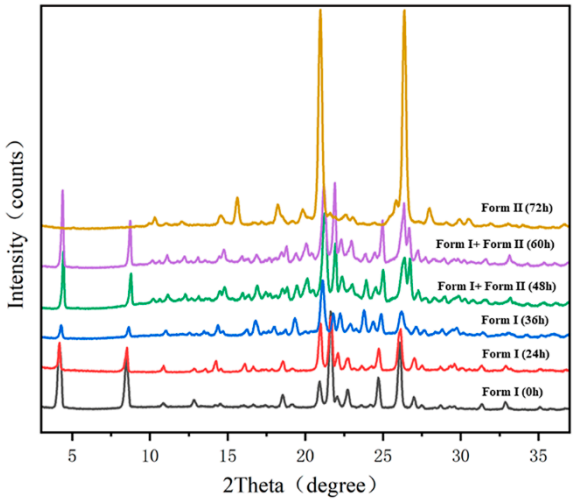

Figure S9. The PXRD patterns of Form I in solvent-mediated phase transformation experiments.

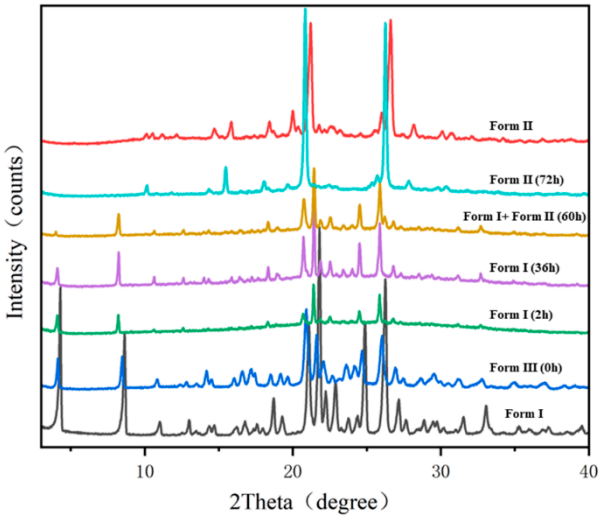

Figure S10. The PXRD patterns of Form III in solvent-mediated phase transformation experiments.